

TRANSMUTATION PERFORMANCE OF MOLTEN SALT VERSUS SOLID FUEL REACTORS (DRAFT)

Björn Becker

*University of California
Nuclear Engineering Department
Berkeley CA 94720-1730 USA
bjorn@nuc.berkeley.edu*

Massimiliano Fratoni

*University of California
Nuclear Engineering Department
Berkeley CA 94720-1730 USA
maxfratoni@nuc.berkeley.edu*

Ehud Greenspan

*University of California
Nuclear Engineering Department
Berkeley CA 94720-1730 USA
gehud@nuc.berkeley.edu*

Keywords: MSR, Molten salt, Transmutation,
TRU

Abstract

This study investigates the transmutation properties of a critical Molten Salt Reactor (MSR) and compares them against those of three types of solid fuel reactors – Lead cooled Fast Reactor (LFR), Sodium cooled Fast Reactor (SFR) and a PWR. A consistent comparison was made of the effect of the different reactor spectra. It was found that the fast reactors spectrum gives the best transmutation performance followed by the MSR and PWR spectra.

A comparison of the fractional transmutations (FT) for an infinitive recycling of actinides (Ac) in the different reactors with a 0.1% loss fraction during reprocessing shows that the MSR has the highest FT due to its high specific power, followed by the SFR and the LFR. Taking into account FT and spectra differences the MSR has preferred transmutation capability.

1. Introduction

The main purpose of this work is to rank the transmutation performance of a critical Molten Salt Reactor for waste transmutation fed only with LWR spent fuel (SF) using the salt mixture LiF (15%), NaF (58%) and BeF₂ (27%). The preferred design, summarized in section 2, consists of a graphite-free pool of molten salt (MS). The third section compares the

transmutation performance of the epithermal-to-fast spectrum MSR against that of fast and thermal neutron spectrum reactors. In the fourth section a comparison is made of the FT of the MSR and two fast reactors. Followed by a quantification of the combined effect of FT and spectrum differences.

2. Molten Salt Reactor

Following is a short overview of the MSR examined in this work.

2.1. Reference reactor

The reference reactor used for this study is similar to the subcritical molten salt ADNA Tier-1 reactor concept proposed by Bowman (1998) for transmutation with two exceptions – it is designed to be critical and it uses a different molten-salt.

The MS carrying the fuel flows through vertical cylindrical channels in graphite blocks arranged in a hexagonal lattice. Channel diameter and lattice pitch are design variables; they determine the ratio between the volume of the graphite and the volume of the molten salt – the C/MS ratio. The core active length is 420 cm. The carrier salt is a mixture of LiF (15%), NaF (58%) and BeF₂ (27%) proposed by Ignatiev et al. (2003) rather than the NaF-ZrF₄ salt proposed by Bowman (1998). The lithium is assumed 100% enriched in ⁷Li. The system is fed continuously with trans-uranium isotopes (TRU) from LWR SF as AcF₃. The power density is 390 W per cm³ of salt in the core (Bowman, 1998). It is also assumed that the volumes of salt in the

core (flow channels) and outside of the core (plena, heat exchangers etc.) are equal and that the MS temperature varies between 600 °C at inlet and 700 °C at the outlet from the core. Fission products (FP) and actinides (Ac) are continuously removed by online reprocessing of a side stream of the MS. Fresh TRU is continuously fed into the core so that, after a long enough operating time, the fuel composition reaches equilibrium. The FP extraction unit capacity is assumed designed to provide the desirable FP's residence time in the core (Fratoni and Greenspan, 2005).

2.2. Constrains

Two constraints are applied in this study: (1) AcF_3 and lanthanide (LnF_3) concentration in the MS should not exceed the solubility limit; the maximum solubility of AcF_3 in LiF (15%), NaF (58%) and BeF_2 (27%) salt at 600°C is 2 mol% (Ignatiev, 2003 and 2005). A conservative constraint imposed is that the combined solubility of AcF_3 and LnF_3 should not exceed 1.5%. (2) k should be about 1.05 in order to compensate for radial neutron leakage from a finite core.

2.3. Computational model

The neutronic analysis is done for a unit cell modeled using MCNP5. This model consists of a finite length hexagonal cell with vacuum axial boundary conditions and reflective radial boundary conditions. Fuel constituents cross sections are taken at 650°C and the graphite scattering kernel at 527°C.

Depletion analysis is done by MOCUP: MCNP5 is used to calculate the neutron flux distribution and effective one-group cross-sections. These cross-sections are supplied to ORIGEN2 that performs depletion calculations. The model is set to seek directly for the equilibrium composition; this composition is independent of the initial state. Full details of the methodology are given in (Fratoni and Greenspan, 2005).

2.4. Graphite-free design

In a recent parametric study reported in (Becker, Fratoni, Greenspan, 2006) it was concluded that the best neutron economy is provided by the $C/MS = 0$ design. The multiplication factor increases as C/MS decreases; the highest k_∞ is obtained for a core without graphite (*Fig. 1*), confirming the findings by Ignatiev et al. (2005). What makes k

peaking at $C/MS=0$ is a significant increase in η , shown in *Fig. 1*, that more than compensates for a slight decline in the parasitic neutron capture (f) and in the non-leakage probability (in the axial direction). With this design the MSR based on LiF (15%), NaF (58%) and BeF_2 (27%) that is fed with and only with TRU from LWR SF can be designed to be critical. The obtained neutron spectrum is epi-thermal to fast (*Fig. 2*). The spectrum exhibits large dips in the 100 eV to 100 keV energy range; they are due to resonances of the sodium and fluorine cross sections.

Additional merits of this graphite-free pool design is that it is the most compact of the MSR and it is not subjected to radiation damage of graphite in the core.

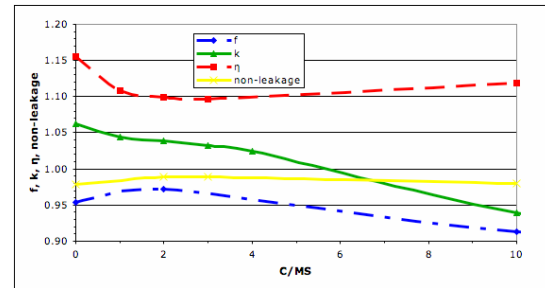


Fig. 1: C/MS dependence of η , f , axial non-leakage probability and k

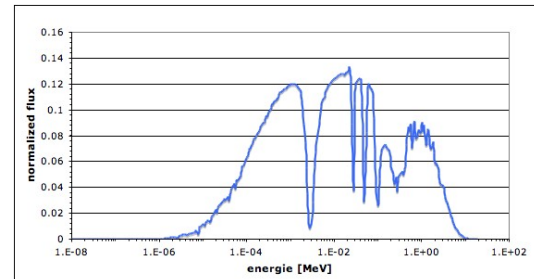


Fig. 2: Normalized neutron flux for $C/MS 0$

2.5. Attainable fractional transmutation

The effect of loss of actinides to the waste stream of the soluble FP removal plant was investigated and the FT estimated. The FT is defined as:

$$FT = 1 - \frac{m_{\text{loss}}}{m_{\text{feed}}} \quad (1)$$

where m_{loss} is the mass of Ac extracted with the FP per GWd and m_{feed} is the mass of Ac fed to the reactor per GWd. This loss is the only Ac removal mechanism besides fission.

For this study it was assumed: (1) 1 year cooled LWR SF from which 100% of the U was

extracted is fed to the reactor; (2) the loss fraction of the Ac that get to the FP reprocessing unit is 0.1%; (3) power density is $390\text{W}/\text{cm}^3$; (4) the reprocessing unit is designed to give a residence time of 1 year for soluble FP and as of Ignatiev et al. (2003) for the others FP; (5) actinide concentration in the core is at the solubility limit of 1.5mol%. A cooling time of the SF as short as 1 year might be possible since complex operations like fuel rod manufacturing are not necessary for the MSR.

It was found that a high fractional transmutation of 99.8% can be reached, while the multiplication factor is higher than $k=1.05$.

3. Homogeneous spectral comparison

The objective of the study reported in this section is to compare the transmutation properties of our preferred MSR with that of fast spectrum reactors as well as with that of the commercially available PWR. Two fast reactor types are considered: LFR (Lead cooled Fast Reactor) and SFR (Sodium cooled Fast Reactor). The transmutation properties compared are radiotoxicity, decay heat, and spontaneous fission neutron yield as a function of time as well as the Pu quality and ^{237}Np inventory. In order to separate the spectrum effect from other design differences the four reactor systems are analyzed using a consistent model that is not realistic for the solid fuel reactors but adequately represents their spectrum. All other reactor parameters like power density, fission product removal strategy and TRU feed composition (50GWd/t HM, 1 year cooling) are kept the same. A homogeneous unit cell model with reflective boundary conditions is used. Actinides, FP, structural materials and coolant are mixed all together conserving their volume fraction in the real system. For all reactors, continuous TRU feeding and extraction and continuous FP removal is assumed, like for the MSR. Even though several values were examined for the fraction, f , of actinides fed that are extracted from the core in the following results are presented only for the $f=1\%$ (FT~99%). All losses in the FP stream are assumed to be included in this fraction of Ac extracted. As it was found that the equilibrium composition is not sensitive to f for values below $f=1\%$.

All unit cells are designed to have $k_{\infty}=1.05$ when at equilibrium composition to allow 5% neutron leakage probability from the finite core. The concentration of fuel in the core is adjusted

to give the target k_{∞} by adjusting the TRU feed-rate, as it is done for the MSR.

3.1. Reactors

MSR

The molten salt reactor considered in this study consists of a pool of molten salt as described above. The power density per unit volume of salt is $390\text{W}/\text{cm}^3$ but since half of the salt volume is outside of the core, half of the total residence time the salt is flowing outside the core. Therefore an effective power density of $195\text{W}/\text{cm}^3$ is considered in this model. The average operating temperature is 650°C .

PWR

The PWR unit cell consists of fuel rods made of an inert matrix fuel, $(\text{TRU})\text{O}_2\text{-ZrO}_2$, with a diameter of 0.819cm and 0.057cm thick Zircaloy clad. The outer diameter of the fuel rod is 0.95cm and a pitch-to-diameter ratio of 1.326 is assumed. Operating temperature is 300°C . The homogeneous mixture consists of 48.42% coolant, 11.64% structure, 38.33% fuel and 1.61% void.

SFR

The sodium reactor considered in this study was developed by ANL as the compact fast burner reactor (Smith et al., 2003). The specific design considered has a very low conversion ratio (C.R.) of 0.25 for actinide transmutation. A single pin in a hexagonal unit cell is modeled. The fuel rod is 0.59cm in outer diameter and the cell pitch is 0.891cm. The cladding of the fuel rods is made of HT-9 alloy and has a thickness of 0.06cm. The fuel is a metallic alloy of TRU and Zr. Average operating temperature of the core is 430°C . The volume fractions of the homogenized unit cell of the different components are (Smith et al., 2003): 50% coolant, 28% structure, 22% fuel.

LFR

The second fast reactor examined in this study is a lead-bismuth eutectic cooled reactor (Cheon et al., 2003), which was designed as a subcritical transmuter. The coolant of this reactor consists of 44.5w% Pb and 55.5w% Bi. The hexagonal unit cell has a pitch of 1.097cm. The fuel pellets are made of an alloy of TRU and Zr and have a diameter of 0.523cm. The smear density of the fuel is 75%. A 0.056cm thick HT-9 alloy cladding is assumed. Operating

temperature of this core is 500°C. The homogenization of this unit cell gives a mixture of 69.59 % coolant, 9.78 % structure, 15.47 % fuel and 5.16 % void.

3.2. Comparison

The neutron spectrum of the different reactors, when the fuel reached its equilibrium composition, is shown in Fig. 3. As expected, the spectra are quite different; whereas the LFR and SFR neutron spectrum peaks around 100 KeV and are negligible below 0.1 KeV, the PWR spectrum has a peak in the thermal energy range as well as in the MeV energy range while the MSR spectrum spreads over the intermediate energy range. Notice that the PWR has a larger component of neutrons above 1 MeV than the other reactors: this is due to the poor slowing down properties of water in the MeV energy range.

Table 1 compares the energy range of the neutrons that cause fissions: almost all the fissions in the PWR are caused by thermal neutrons. In the MSR fissions are induced mainly by intermediate energy neutrons while in a LFR and SFR fission causing neutrons are fast to intermediate. Table 2 gives a comparison of Ac recycling time, mass fissioned per GWd, Ac concentration, average neutron flux, effective one group fission cross section and the ratio of the one group fission to absorption cross sections of actinides. The concentrations needed to obtain $k_{\infty}=1.05$ are different. The PWR needs the lowest concentration, followed in order by MSR, LFR and SFR. Since the Ac concentrations are different, their recycling times are also different.

The ratio of fission to absorption cross sections varies with the spectrum. For the lead and sodium cooled reactors about 50% to 53% of absorbed neutrons induce a fission. This ratio is only about 40% for the MSR and PWR. The equilibrium composition of the MSR is much

closer to those of the SFR and LFR than to that of the PWR (Fig. 4). The Pu makes 73% of the actinides of the MSR versus 82% in the SFR, 83% in the LFR, 40% in the PWR, and 91% in the feed. However, the concentration of higher actinides in the MSR is closer to that of the PWR and smaller for the fast reactors. All equilibrium compositions compared to the feed composition show a similar trend: ^{239}Pu and ^{237}Np are reduced due to fission and neutron capture while ^{243}Am and ^{244}Cm to ^{248}Cm build up. ^{244}Cm builds up the most. The fraction of ^{240}Pu in the discharged Pu is the lowest for the PWR.

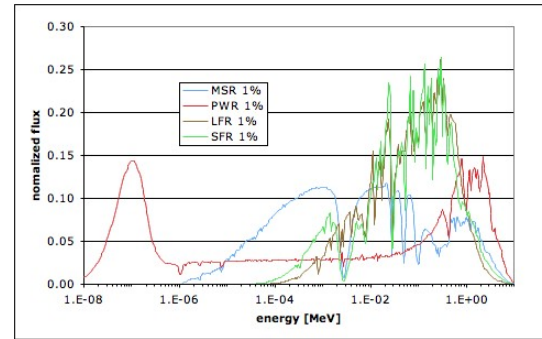


Fig. 3: Comparison of neutron spectrum for MSR, PWR, LFR, SFR

Table 1: Percentage of fast, intermediate and thermal fission for MSR, PWR, SFR, LFR

Reactor	Fast fission >100keV	Epithermal fission 0.625eV - 100keV	Thermal fission <0.625eV
PWR	1%	5%	94%
MSR	4.5%	95.3%	0.2%
SFR	34.6%	65.4%	0.0%
LFR	41.5%	58.5%	0.0%

Table 2: Comparison of Ac recycling time, fissions per GWd, concentration, neutron flux, σ_f and σ_f/σ_a ratio for MSR, PWR, SFR, LFR

Reactor	PWR	MSR	SFR	LFR
Recycling Time [years]	71.56	138.85	385.22	247.12
Fission rate [g/GWd]	1007.9	1006.9	1011.9	1012.3
Actinides concentration [at%]	0.17	0.36	1.55	1.25
Actinides concentration [mol/cm ³]	2.06E-4	4.12E-4	11.7E-04	7.49E-04
Neutron flux [n/s/cm ²]	2.17E+15	4.04E+15	6.95E+15	1.28E+16
σ_f [barn]	4.06E+01	5.95E+00	1.92E+00	9.94E-01
σ_f/σ_a	0.396	0.392	0.499	0.531

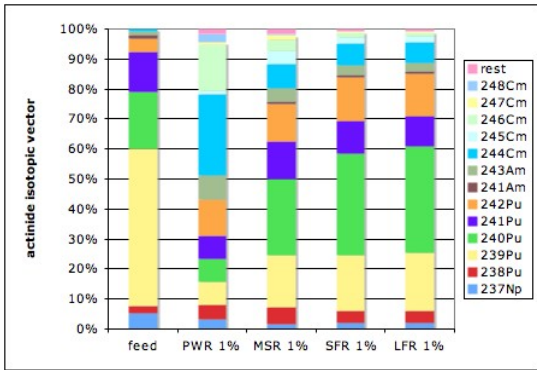


Fig. 4: Comparison of actinides equilibrium versus feed

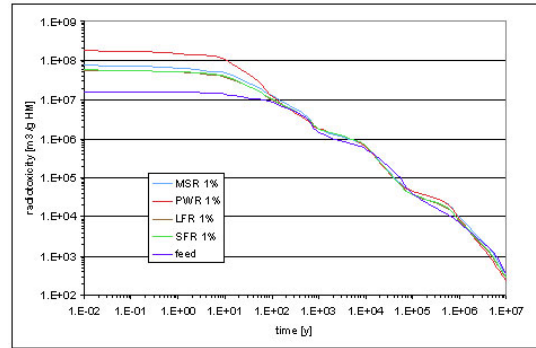


Fig. 5: Comparison of radiotoxicity time evolution per gram Ac for feed, MSR, PWR, LFR, SFR

Radiotoxicity

The radiotoxicity of the actinides discharged from the different reactors is defined by the ingestion-toxicity index. This index gives the volume of water in which the discharged TRU must be diluted so that drinking this water will not cause a cumulative radiation dose exceeding 0.5 rem/year. A relative timescale is used to describe the radiotoxicity: time zero corresponds to the moment of discharge of actinides from the reactor. Since FT is the same for all reactors the index is given per gram of discharged actinides. In the first 100 years the radiotoxicity of actinides from the PWR is the highest. The radiotoxicity is about one order of magnitude higher than that of the TRU feed (Fig. 5). The radiotoxicity of Ac from the MSR is about half of the one from the PWR while the radiotoxicity of Ac from the LFR and the SFR, is slightly smaller. After this period the radiotoxicity of Ac from the reactors and from the feed TRU are very close. None of the examined spectra shows a clear advantage.

The difference in the radiotoxicity in the short time range is primarily due to the difference in the concentration of heavy actinides with short half-life including ^{242}Cm and ^{244}Cm (Fig. 6). After 100 years of cooling these actinides decay to such a low concentration that their contribution to the radiotoxicity becomes insignificant. After this early period Pu dominates the radiotoxicity. Since the concentration of Pu in the PWR equilibrium core is relatively small, the contribution of Pu to the radiotoxicity is smaller but the contributions of the higher actinides make the total radiotoxicity from PWR comparable to that of the other systems (Fig. 7).

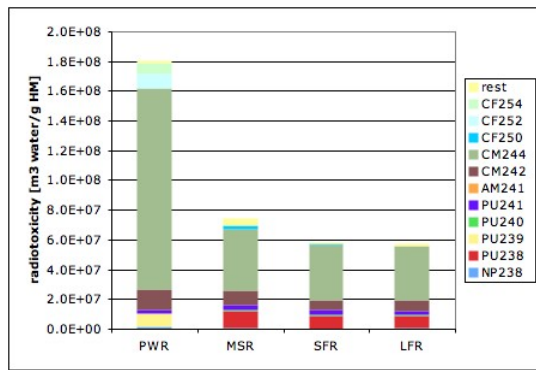


Fig. 6: Comparison of radiotoxicity per gram Ac at discharge for MSR, PWR, LFR, SFR

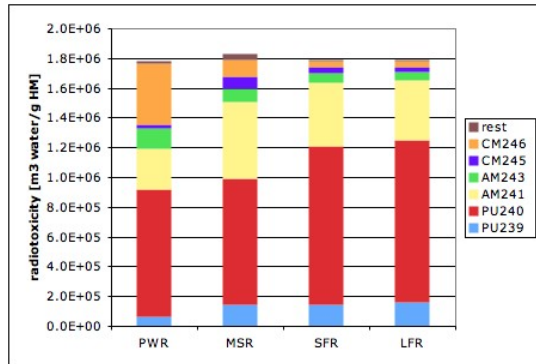


Fig. 7: Comparison of radiotoxicity per gram Ac 1,000 years after discharge for MSR, PWR, LFR, SFR

Decay heat

The decay heat time evolution (Fig. 8) shows a similar behavior as the radiotoxicity: actinides that are removed from the PWR have the highest decay heat in the first 100 years. Their decay heat is more than one order of magnitude higher than the decay heat of the feed

and twice as high as the decay heat of actinides from a MSR. Actinides from the LFR and from the SFR have the lowest decay heat (besides the feed). Afterwards, there is no preferred spectrum: decay heat of Ac from all reactors and the feed are close. In a short period after discharge, the decay heat is dominated by the short-lived ^{242}Cm and ^{244}Cm and for PWR also ^{252}Cf and ^{254}Cf . In the 100 to 1,000 years time range ^{238}Pu , ^{240}Pu , ^{241}Am and ^{244}Cm make the dominant contribution. The relative contribution of ^{244}Cm is larger while that of ^{241}Am is smaller for PWR than for the other reactor types.

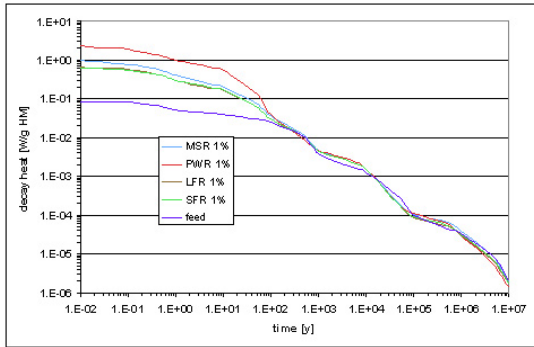


Fig. 8: Comparison of decay heat time evolution per gram Ac for feed, MSR, PWR, LFR, SFR

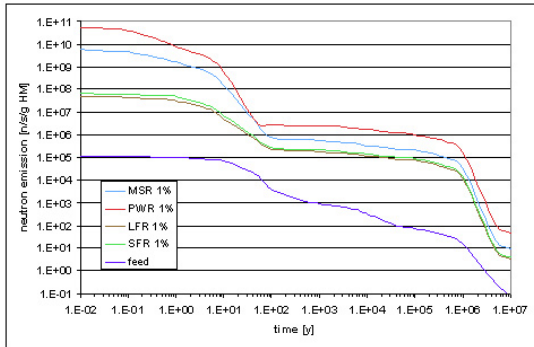


Fig. 9: Comparison of neutron emission time evolution per gram Ac for feed, MSR, PWR, LFR, SFR

Spontaneous neutron emission

The differences in the spontaneous neutron emission are significantly larger than the differences in the radiotoxicity and decay heat. The neutron emission per gram Ac from PWR is up to six orders of magnitude higher than the emission of the feed. The neutron emission of Ac from the MSR is five orders of magnitude higher while the neutron emission of Ac from LFR and SFR are three orders of magnitude higher. After 100 years the difference between the different

reactors becomes smaller but there is still one order of magnitude difference between the PWR compared to LFR and SFR. The MSR is in between. The reason for these differences is due to the build up of higher actinides in a thermal spectrum, which are main contributors to the neutron yield. Short after discharge ^{254}Cf ($T_{1/2}=60.5\text{d}$) and ^{252}Cf ($T_{1/2}=2.65\text{y}$) are main contributors while afterwards, ^{246}Cm ($T_{1/2}=4.76\text{ky}$) and ^{248}Cm ($T_{1/2}=348\text{ky}$) are the main contributors.

^{237}Np concentration

The concentration of ^{237}Np is an important measure of long-term environmental impact of a repository like the Yucca Mountain Repository (YMR). ^{237}Np is a long-living radionuclide ($T_{1/2}=2.14 \cdot 10^6$ years) with a high mobility and might be the dominant contributor to long-term radioactivity release from the YMR. The sum of the concentrations of ^{237}Np and of its shorter living precursors ^{241}Pu , ^{241}Am and ^{245}Cm give the cumulative concentration of ^{237}Np , which is quite constant in the first 10,000 years after discharge of actinides from the reactors. The cumulative ^{237}Np concentration of the MSR is the highest – 19.4% of the Ac vector, followed by the SFR (15.8%), LFR (15%) and PWR (12.5%).

Proliferation resistance

Enhanced proliferation resistance of the plutonium discharged from the transmuter reactors is obtained by reducing its fissile isotopes fraction, increasing its specific decay heat and increasing its specific spontaneous neutron yield.

MSR has the highest fraction of fissile Pu, followed in order by the PWR and the fast reactors (Table 3). On the other hand, Pu from the fast reactors has the lowest decay heat and neutron yield, followed by the MSR and the PWR. The overall differences, though, are within a factor of 2.

Table 3: Fissile fraction of Pu vector, decay heat and neutron yield per gram Pu (PWR, MSR, SFR, LFR)

	PWR	MSR	SFR	LFR
Fissile fraction	39.0%	40.9%	35.5%	35.8%
Decay heat [W/g]	6.7E-02	4.5E-02	3.1E-02	3.0E-02
Neutron yield [n/s/g]	1.8E07	1.6E07	1.2E07	1.2E07

Power density

The effect of the power density on the above discussed transmutation performance was investigated parametrically. It was found that the power density effect on radiotoxicity and decay heat is very small. It is higher on the spontaneous neutron emission in the first years after discharge of actinides; afterwards the effect is negligible. The main effect of higher power density is a reduction of the recycling time since actinides are faster transmuted (*Table 4*). Thus compared on an absolute timescale, in the first period after discharge the transmutation indexes are lower for a higher power density.

Table 4: Neutron flux and recycling time as function of power density in MSR

Power density	104 W/cm ³	195 W/cm ³	400 W/cm ³
Flux [n/cm ² /s]	2.15E+15	4.05E+15	8.36E+15
Recycling time	23.8 y	12.24 y	5.63 y

4. Comparison of fractional transmutation

The effectiveness of transmutation depends on the reactor spectrum, as shown in the previous section. However, the transmutation performance also depends on the waste mass reduction, measured by the FT, that is reactor type dependent. The entire fuel cycle and realistic models of the different reactors have to be considered in order to estimate the loss of actinides for, practically, an infinitive recycling. Since the thermal PWR spectrum has a weaker transmutation performance, the MSR is only compared against the LFR and SFR. The LFR of the previous section is considered, while for the SFR, the ANL design having a C.R of 0.0 (Smith et al., 2003) was used; 1/7th of its core loading is replaced each cycle.

For all systems a loss rate of 0.1% of the actinides going through the FP extraction process is assumed. *Table 5* summarizes the characteristics of the different systems. The Ac loss rate of the SFR was calculated by assuming that 1/7 of the EOC HM inventory goes through the reprocessing every cycle. The loss rate of the LFR was taken to be the loss rate per cycle given in the reference (Cheon et al., 2003).

The MSR specific inventory is less than a third of the specific inventory of the FR. This is

a result of the lower Ac concentration needed to obtain criticality and a high power density possible with liquid fuel. The low specific inventory reduces the MSR loss rate since less Ac go through the reprocessing per recycle. However, the recycling time of the MSR is the shortest. Nevertheless, the net effect is that the overall loss rate per GWd is the smallest for the MSR, followed by the SFR and LFR. That is, the MSR has the highest FT.

The combined effect of the different FT and spectra is summarized in *Table 6*. The radiotoxicity, decay heat, neutron yield and ²³⁷Np concentration brought in this table are measured one year after discharge from the MSR, SFR and LFR and are given as ratio of those of the MSR.

Due to the high FT, Ac discharged from the MSR have the lowest radiotoxicity, decay heat and ²³⁷Np concentration followed by the SFR and the LFR. However, the MSR has the highest neutron emission rate followed by the SFR and the LFR.

5. Conclusion

The studies presented in this work show that the MSR epi-thermal to fast spectrum has a medium ranked transmutation performance due to a stronger build up of higher actinides compared to fast reactors. The radiotoxicity, decay heat and neutron emission is higher during a short period after the discharge of actinides. In a longer timeframe, significant differences can only be noticed for the neutron emission. In addition the MSR has the highest ²³⁷Np concentration and a medium proliferation resistance.

However, assuming an infinitive Ac recycling a comparison of the FT indicates that the MSR has a higher FT than the FR. This is mainly due to the high specific power of the MSR. The combined spectrum and FT effects make the radiotoxicity, decay heat and ²³⁷Np release from the MSR smaller than those of the FR. The spontaneous fission neutron yield is the highest for the MSR.

MSR is a promising option for LWR waste transmutation. Further investigations of the MSR need to identify proper reflector and containment materials and design; to calculate reactivity coefficients; and to address control requirements, reactor safety and economics.

Table 5: Comparison of models for MSR, SFR and LFR

	MSR	SFR (Smith et al., 2003)	LFR (Cheon et al., 2003)
Coolant	15LiF + 58NaF + 27BeF ₂	Na	LBE
Fuel Type	Liquid TRU F ₃	Metallic TRU in ZR matrix	Metallic TRU in ZR matrix
Number of cycles	Continuous	7	6
Length of cycle	--	6 months	6 months
Capacity factor	100%	85%	75%
Power density	390W/cm ³	332.54 W/cm	181.41W/cm
Total reactor power [MWth]	750	840	840
FP residence time	12 months (Soluble FP)	49.4 months	48 months
HM specific inventory	692 kg/GW	3001 kg/GW (BOC) 2842 kg/GW (EOC)	2500 kg/GW (BOC) 2354 kg/GW (EOC)
Loss rate	1.89 g/GWd	2.26 g/GWd	2.87 g/GWd

Table 6: Fractional transmutation and radiotoxicity, decay heat, neutron emission and ²³⁷Np concentration of discharged Ac 1 year after discharge from MSR, SFR and LFR normalized to the MSR

	MSR	SFR	LFR
FT	99.85%	99.78%	99.71%
Radiotoxicity	1	1.19	1.53
Decay heat	1	1.11	1.46
Neutron emission	1	0.043	0.039
²³⁷ Np and precursors	1	1.19	1.50

References

Bowman C.D. (1998), "Accelerator-Driven Systems for Nuclear Waste Transmutation," Annual Review of Nuclear and Particle Science, Vol. 48, December

Becker B., Fratoni M., Greenspan E. (2006), "Feasibility of a Critical Molten Salt Reactor for Waste Transmutation," INES-2, Yokohama, Japan, Nov. 27-30

Cheon M. et al. (2003), "Reduction of TRU Toxicity in LWR-Spent Fuel by Reference ATW System with LBE-Cooled Subcritical Transmuters," Global 2003, New Orleans, LA, Nov. 16-20

Fratoni M., Greenspan E. (2005), "Transmutation Capability of Molten Salt Reactors Fed with TRU from LWR," AWRIF-2005, Oak-Ridge, TN, February 16-18.

Ignatiev V. et al. (2003), "Reactor Physics & Fuel Cycle Analysis of a Molten Salt Advanced Reactor Transmuter," ICAPP'03, Córdoba, Spain, May 4-7.

Ignatiev V. et al. (2005), "Integrated Study of Molten Na,Li,Be/F Salts for LWR Waste Burning in Accelerator Driven and Critical System," GLOBAL 2005, Tsukuba, Japan, Oct 9-13.

Smith M. A. et al. (2003), "Physics and Safety Studies of Low Conversion Ratio Sodium Cooled Fast Reactors," GLOBAL 2003, New Orleans, LA, Nov 16-20